

Perinatal Journal 2025; 33(2):594-602

https://doi.org/10.57239/prn.25.03320065

Influence of magnetron DC sputtering conditions and annealing on the structural, morphological, and optical properties of AG/AU thin films

Sinai Mohan Khalil¹, Ahmed Hmeed Wanas^{1*}

¹Department of Physics, College of Education, University of AL-Qadisiyah, Qadisiyah, Iraq

Abstract

This study examined how sputtering current and annealing affect the structure, surface morphology, and composition of Ag/Au thin films that are deposited by DC sputtering. X-Ray Diffraction (XRD) analysis showed an increase in the sputtering power of the bell jar. Increasing the sputtering current from 10 mA to 20 mA improved the crystallinity, increased crystallite size and reduced lattice strain while annealing improved the sputtered film and structural uniformity. The surface is a bit different as observed from the FESEM images. With low sputtering current of 10 mA, the as-deposited film exhibited heterogeneous structures of mixed rod-like and spherical nanoparticles. Increasing currents caused larger spherical grains. After annealing, the films were able to become more continuous and less porous. Therefore, the film surfaces became denser and more homogeneous. The EDX analysis indicates lower content of Au as compared to Ag under similar deposition conditions. When the sputtering current was increased, the Au content increased too. This means that the deposition parameters are very important to consider.

Keywords: Ag/Au thin films, DC sputtering, Annealing, FESEM

1. Introduction

Plasma sputtering is the base for the preparation of thin films for many sophisticated researches, due to the unique properties of the films prepared, for their use in technology in the field of applied physics and nanotechnology [1]. Cold plasmas are a medium rich in energetic electrons, reactive ions, and neutral species with gas temperatures close to ambient. Their microsurface processes make them suitable for materials engineering [2]. Sputtering glow discharge plasmas is a basic configuration for experimental and applied purposes, among the various plasma systems. Sputtering is a physical vapor deposition (PVD) process for depositing thin films. When ions are accelerated towards a target material in a lowpressure environment, atoms are scattered and deposited on a substrate [4]. Sputtering systems that you control are great for using as deposition of thin films, etching, and surface treatment. The flexibility in designing the microstructure and the adhesion property of deposited film can be altered by these variables. Although sputtering is widely practised, a understanding of plasma-material interactions, the influence of different species over deposition efficiency and conditions to obtain high

quality defect free films are still sought after. Other than that, the impact of plasma parameters on the prepared films' physical properties such as pressure, discharge power, and substrate temperature are investigated.

Sputtering methods make thin films that have special nanoscale features that are different from the bulk properties. Films are used in the manufacture of optoelectronic devices, sensors, ICs and photovoltaic (PV) systems.

Stansfield et al. in 2018 studied the deposition of Au, Ag and Ag-Au alloy nanocrystal thin films at the water-toluene interface. The level of toluene in the solution was varied to create an alloy. This caused metallic films to become non-metallic, with increasing Au content. The films were taken to different substrates and characterized using AFM, UV-Vis, XRD, XPS, SEM and TEM. The results showed reproducible changes of structural and transport properties Surya and others made ultra-thin Au-Ag-Au tri-layer films deposited thermally on flexible substrates. The scientists researched the mechanical, optical, and electrical properties. They saw that the ~8 nm thickness provided high transparency ~62%

and conductivity. The films showed stable sheet resistance, high carrier concentration and mobility. Kim et al (2023) [10] looked into the thermal conduction of thin Au and Ag films deposited on SiO2 substrates with Ti adhesive layers. In this study, the size effects of metal permittivity and the influence of the Ti layer on plasmon transport were analyzed. It was found that the plasmon conductivity reached ~20% of the electron contribution. The authors of study [11] Yergaliyeva et al (2023) synthesized composite TiO2 thin films containing Ag, Au, and Ag/Au nanoparticles by RF magnetron sputtering. Annealing in argon induced crystallization.

Earlier studies have primarily concentrated on the deposition of either a single metal thin film or Au–Ag alloys at limited sputtering conditions without much focus on the combined impact of sputtering parameters and annealing in situ deposition on the deposit characteristics. By observing Au–Ag thin films at various sputtering currents and studying the effect of annealing on the geometry of films, this study covers these gaps. This work is to investigate the effect of different sputtering currents and post-upon annealing on the structural, surface morphology, and composition of Ag/Au alloy thin films by DC sputtering.

2. Experimental

Gold and silver were deposited by a DC co-sputtering glow discharge system. The apparatus included a vacuum chamber which has the size of the diameter of 30 cm and height of 40 cm. The chamber used a combination of rotary and diffusion pumps to bring down the base pressure to $1.0 \times 10 - 6$ mbar.

For the experiment, use of two magnetrons with gold (99.9%) and silver (99.9%) targets of diameter 5 cm was done. As schematically shown in Figure 1, the targets were mounted looking downward at 450 towards the centre of the anode. Because this process was sputtering, the AR flow was adjusted for the pressure settings using the needle valve.

The material was kept under 2 mbar pressure in argon (99.9%). Pre-cleaned glass substrates were used to carry out deposition using different sputtering currents of 10, 15, and 20 mA. We used digital mustimeters to track the voltage and current during the deposition.

The deposited films were analysed using X-ray diffraction (XRD, SHIMADZU-6000) with Cu-K α radiation (λ = 1.5406 Å) using a voltage of 40 kV. Field emission scanning electron microscopy (FESEM, Inspect F-50 FEI Com.) is used to study the surface morphology, while elemental composition is studied by (EDX).

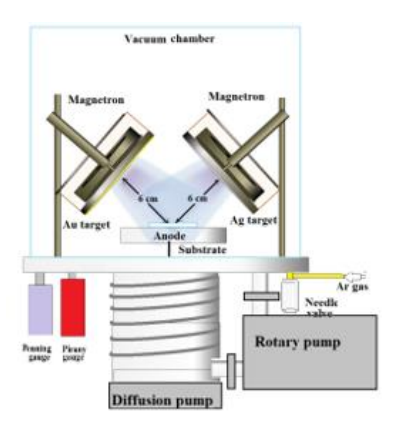


Figure 1: Scheme of the co-sputtering system

3. Results and Discussion

Figure 2 shows the X-Ray Diffraction (XRD) patterns of Ag/Au thin films prepared by DC sputtering at an operating pressure of 2 mbar using different currents of 10, 15, and 20 mA. At 10 mA, the sample exhibits an amorphous structure. While, the others exhibit diffraction peaks consistent with the face-centered cubic (FCC) structure, with the most intense occurring approximately reflection at corresponding to the (111) plane, and a weaker peak at approximately 44°, corresponding to the (200) plane, corresponding to both gold and silver structures. Since they have closely dimension cubic structures, their diffraction angles are so similar that they cannot be distinguished, especially for broad diffraction lines. The dominance of the (111) peak in all patterns indicates a strong preferred growth direction along this plane, which is common in cubic structures due to the highest surface atomic density. No additional diffraction peaks associated with secondary phases such as oxides were observed due to vacuum deposition.

One can observe that increase in the sputtering current, crystallinity improves significantly. When the intensity is increased to 15 mA, the peak in the (111) direction becomes steeper and more intense. Additionally, the peak in the (200) direction appears

clearer, suggesting grain growth and partial strain relaxation. The (111) peak becomes the most pronounced and sharpest in the samples at the highest current (20 mA), the decrease in amplitude of the peak indicates a decrease in crystallite size and density of defects. The (111) peak position does not change significantly; this can be attributed to alloy composition. The peaks' gradual shifting, which can be attributed to structural amelioration and the disintegration of lattice strain, results in a minor adjustment in the lattice modulus.

Figure 3 shows the X-Ray Diffraction (XRD) patterns of Ag/Au mixed thin films deposited at different sputtering currents, and subsequently annealed in air. All annealed films retain the cubic structure with the dominant (111) reflection. No additional peaks are attributed to oxide phases, indicating that air annealing does not result in detectable oxidation within the measurement sensitivity. Annealing results in increased diffraction peak intensity compared to the deposited films discussed previously. The FWHM of the (111) line gradually decreases with the sputtering current.

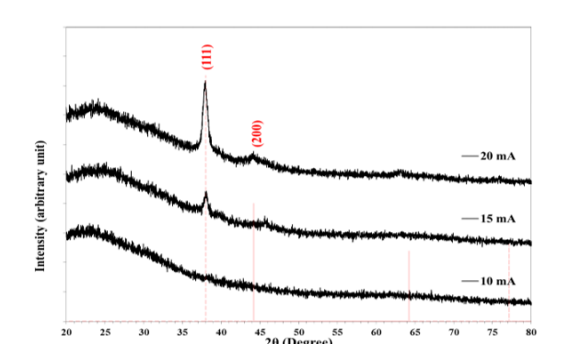


Figure 2: XRD patterns of the as-deposited Ag/Au thin films deposited at different sputtering currents

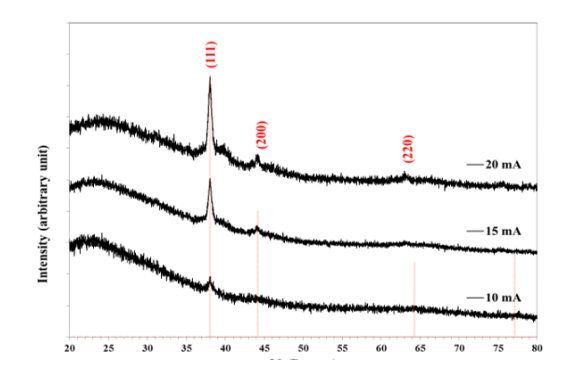


Figure 3: XRD patterns of the annealed Ag/Au thin films deposited at different sputtering currents

The interplane distances (d_{hkl}) specific to the Miller indices (hkl) direction were calculated using the Bragg's relation based on the peak positions [12]:

$$n \lambda = 2 d_{hkl} \sin \theta \qquad \qquad \dots \tag{1}$$

where n is the diffraction order, λ is the wavelength of the x-ray, and θ is the diffraction angle.

The crystallite size (D) was calculated using the Scherrer's equation based on the width of the diffraction peaks at half-intensity (FWHM) [13]:

$$D = \frac{0.89\lambda}{\beta \cos \theta} \qquad \dots \tag{2}$$

where, β is the diffraction line breadth in radians.

Lattice strain refers to the deformation of crystal lattice due to various intrinsic and extrinsic factors. Strain can significantly influence the properties of the deposited films. Lattice strain (ϵ) is often determined using XRD by analyzing peak broadening. A simplified approach to calculate strain is given by the relation:

$$\varepsilon = \frac{\beta}{4\tan\theta} \qquad(3)$$

As shown in Table 1 the crystallite size of the asdeposited samples increased from 9.4 nm at 15 mA to 11.4 nm at 20 mA sputtering current. While, the lattice strain gradually decreased from 3.76×10^{-3} to 3.02×10^{-3} with increasing current. The annealed sample increased from 9.2 nm at 10 mA to 11.6 nm at 20 mA sputtering current. While, the lattice strain decreased from 3.78×10^{-3} to 2.97×10^{-3} with increasing current. These trends confirm that both increasing current and annealing promote grain growth and reduces defect-induced strain.

The peak positions change slightly with increasing current. For the (111) reflection, 2θ shifts slightly to lower angles, corresponding to a gradual increase in $d_{(111)}$. This slight lattice expansion with the sputtering current, along with the decrease in microstrain, is consistent with annealing-assisted lattice strain relaxation and improved atomic packing. Comparing the annealed with the as-deposited films, three major improvements are observed: (1) narrower diffraction lines and higher intensity, indicating larger grain sizes; (2) reducing lattice strain extracted from line broadening, reflecting relaxation of lattice strain; and

(3) a slight shift of the main peak toward higher 2θ values in the higher-current depositions, resulting in

a slight indicates on decrease in the lattice constant.

	I (mA)	2θ (Deg.)	FWHM (Deg.)	d _{hkl} Exp.(Å)	C.S (nm)	hkl	2×10-3	
	10	Amorphous						
As- deposited	15	38.0141	0.8912	2.3652	9.4	(111)	3.6766	
	20	38.0200	0.7339	2.3648	11.4	(111)	3.0276	
		44.1153	1.0485	2.0512	8.2	(200)	4.2401	
Annealed	10	37.6598	0.9168	2.3866	9.2	(111)	3.7862	
	15	37.9976	0.7720	2.3662	10.9	(111)	3.1850	
	20	38.0941	0.7220	2.3604	11.6	(111)	2.9778	

The crystal can be formed at various structures according to Bravais lattice. As an example, gold and silver have a cubic structure. The lattice parameter (a) for cubic structure is determine based on the d_{hkl} values and miller indices (hkl) using the relation [14]:

$$\frac{1}{d^2} = \frac{h^2 + k^2 + l^2}{a^2} \qquad \dots (4)$$

Figure (4) shows the variation of the lattice constant, grain size, and lattice strain with the sputtering current for the as-deposited and annaeled Ag/Au thin films. The lattice constant values are within those reported for silver and gold (Ag-0.409, Au-0.408 nm) according to JCPDS 04-0783 and 04-0784, respectively [15]. The figure shows an increase in the lattice constant in both groups with the sputtering current. This is due to the removal of lattice strain with the improvement of crystallinity of the deposited samples, as a result of improved crystallization with increasing sputtering current. Higher currents increase the energy of the deposited particles, facilitating the rearrangement of atoms into their ideal lattice positions. The figure also shows an increase in crystallite size, with opposite behavior of the lattice strain values with increasing sputtering current. These results can be explained based on the dynamics of growth during sputtering. As the sputtering current increases, the flow rate of atoms toward the surface increases, and their average kinetic energy increases, giving them greater ability to diffuse over the surface and reach more stable energy positions. This, in turn, promotes crystallization and reduces strain. The increased grain size also means a lower proportion of atoms at grain boundaries, the areas where most internal strain are concentrated, which explains the observed decrease in lattice strain values.

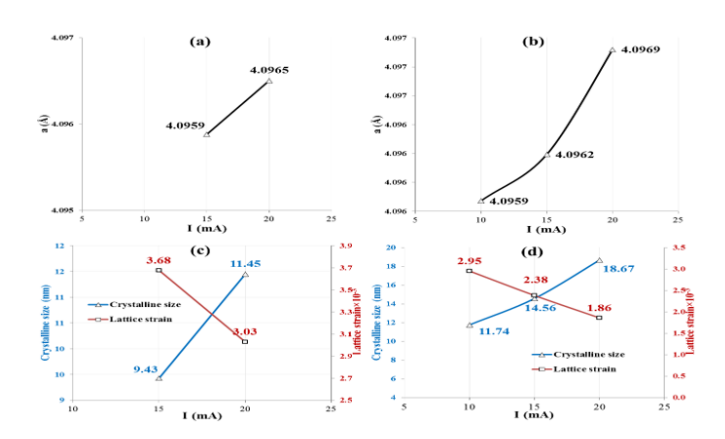


Figure 4: Variation of lattice constant for (a) as-deposited and (b) annealed Ag/Au thin films; Variation of crystaalite size and lattice strain with sputtering current for (c) as-deposited and (d) annealed Ag/Au thin films

The FESEM images of the as-deposited Ag/Au thin films deposited at different sputtering currents, shown in Figure 5, were taken at two different magnifications. Sputtering current causes notable differences in surface morphology and distribution of particle sizes. We can take a look at the film surface. At the 10mA level, we see two types of particles. These are elongated rod-like types. Their growth length is up to 490 nm while the width is 76 nm. Further, we can also see partially merged spherical nanoparticles. These have a growth diameter of 20 to 50 nm. This indicates dual structural phases. So we may have somewhere in between silver-rich and gold-rich nanoparticles. They may have crystallized with different growth patterns. The different distributions had gaps between clusters and didn't completely cover the surface indicating little atomic movement at the low sputternig currents.

When the current goes up to 15 mA, the surface looks

more like a tightly packed lump. The nanoparticles are primarily spherical in shape and have a diameter that ranges from 30 to 60 nm. Furthermore, they showed more uniformity compared to those found in the 10 mA film. With the growth of the films, greater

surface diffusion and atomic mobility take place resulting in isotropic granular growth and better film coverage. A lower void ratio shows a more continuous and cohesive film..

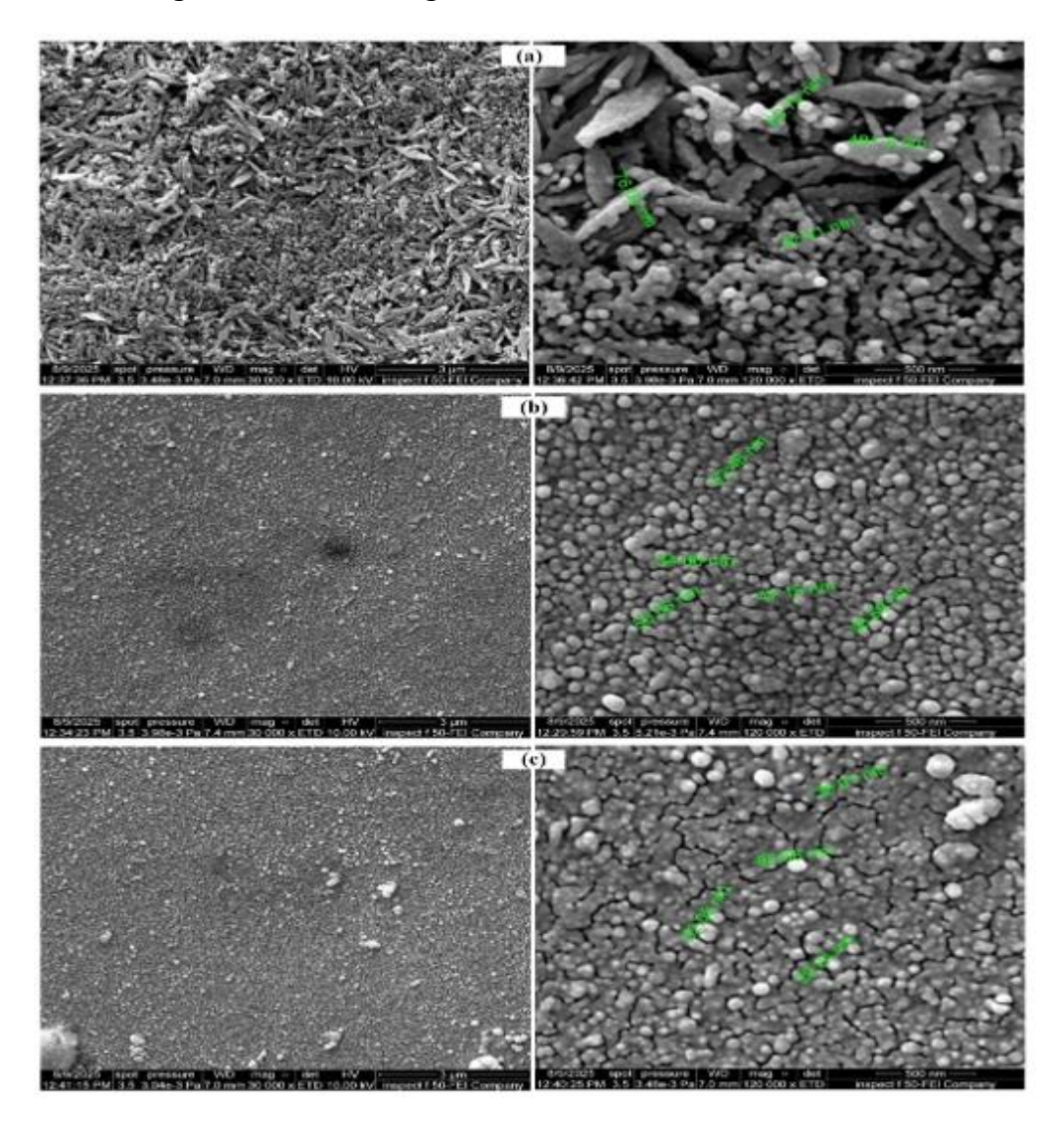


Figure 5: FESEM images at two magnifications of the as-deposited Ag/Au thin films deposited at different sputtering currents (a) 10 mA, (b) 15 mA, and (c) 20 mA

At the highest current of 20 mA, the morphology retains a spherical granular structure but with larger average particle sizes, some reaching over 100 nm. The grains saparate with clearly visible cracks between the particles. These defects are due to the increased deposition rate at low temperature. Some larger agglomerates are also present as a result of localized merging of smaller grains. These morphological observations are consistent with the XRD results, where increasing the sputtering current

showed enhanced crystallinity.

Figure 6 shows the FESEM images at two different magnifications of the annealed Ag/Au thin films deposited using different sputtering currents. Clear changes in surface morphology and particle size distribution were observed with increasing the sputtering current. It also shows marked differences between the states of before and after annealing. The grain observed with particle growth and merged

together, indicating atomic rearrangement and a reduction in surface defects.

The two phases that appeared before annealing were merged to form a single, more homogeneous phase after annealing, with a slight increase in grain size and a decrease in porosity, indicating a clear improvement in the degree of crystallinity. Increasing the current to 15 mA changed the surface morphology to a more pronounced granular structure. Isotropic grain growth and a clear improvement in film coverage were also observed.

At the highest sputtering current (20 mA) the surface retained its spherical grain structure, but with a clear increase in particle size, with some reaching over 200 nm. The grains also became more separated

compared to lower currents, which may be attributed to the increased energy of the deposited atoms, which promotes grain growth at the expense of the density of the nucleation centers.

In general, all samples annealed at 2 mbar showed improved crystallinity and grain size growth compared to the unannealed state under the same deposition conditions. This is attributed to the role of annealing in increasing the kinetic energy of the atoms at the surface, allowing them to move to more stable lattice positions and reducing internal strain and structural defects. These results are consistent with the results obtained from X-ray diffraction patterns. This result is consistent with the researcher [16].

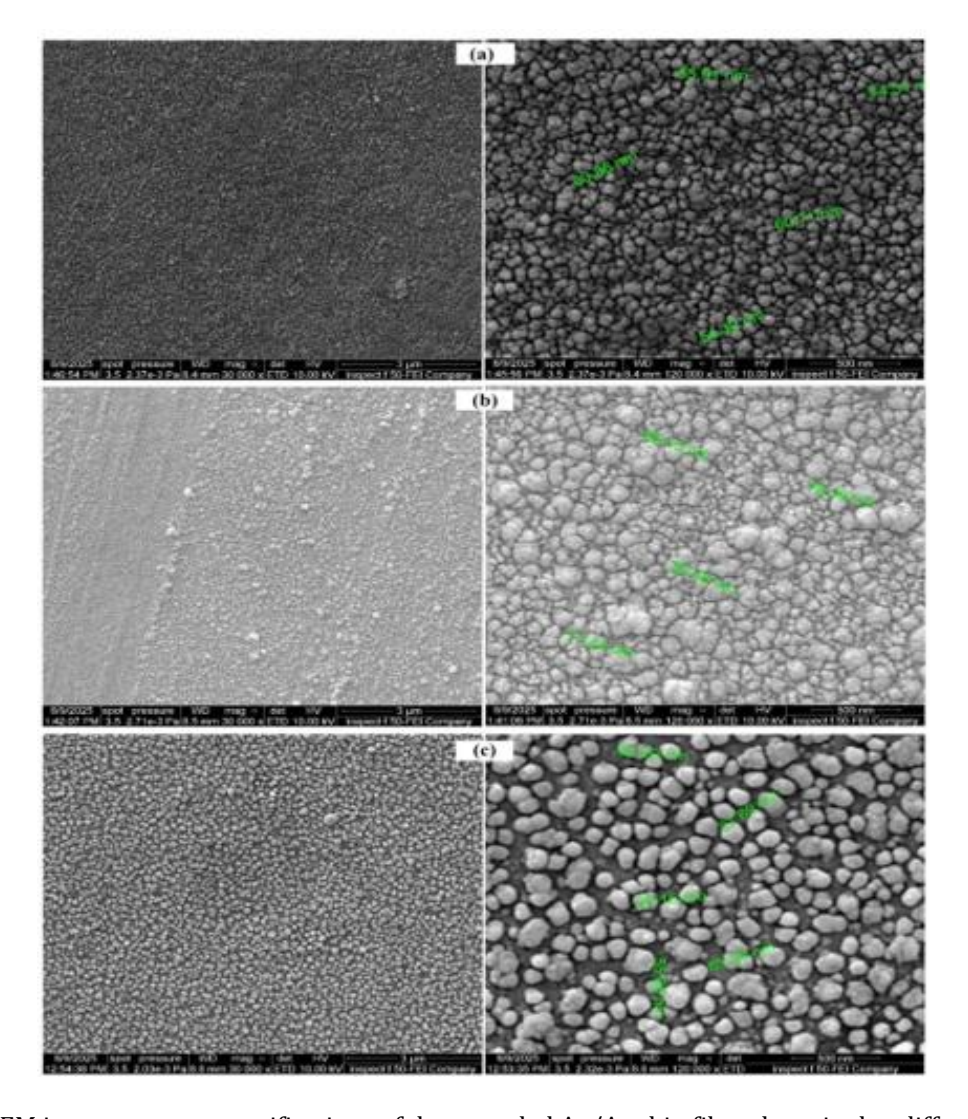


Figure 6: FESEM images at two magnifications of the annealed Ag/Au thin films deposited at different sputtering currents (a) 10 mA, (b) 15 mA, and (c) 20 mA

The elemental compositions of the Ag/Au thin films deposited at different sputtering currents were confirmed by EDX analysis. Figures 7 shows the EDX analysis of the Ag/Au thin films deposited at different sputtering currents for the as-deposited and annealed samples. The patterns show peaks of gold

and silver, in addition to the presence of silicon and other minor elements of the glass substrate. The intensity of the gold and silver peaks increases with increasing sputtering current at different rates, indicating an increase in their content in the prepared films. These results are supported by the XRD.

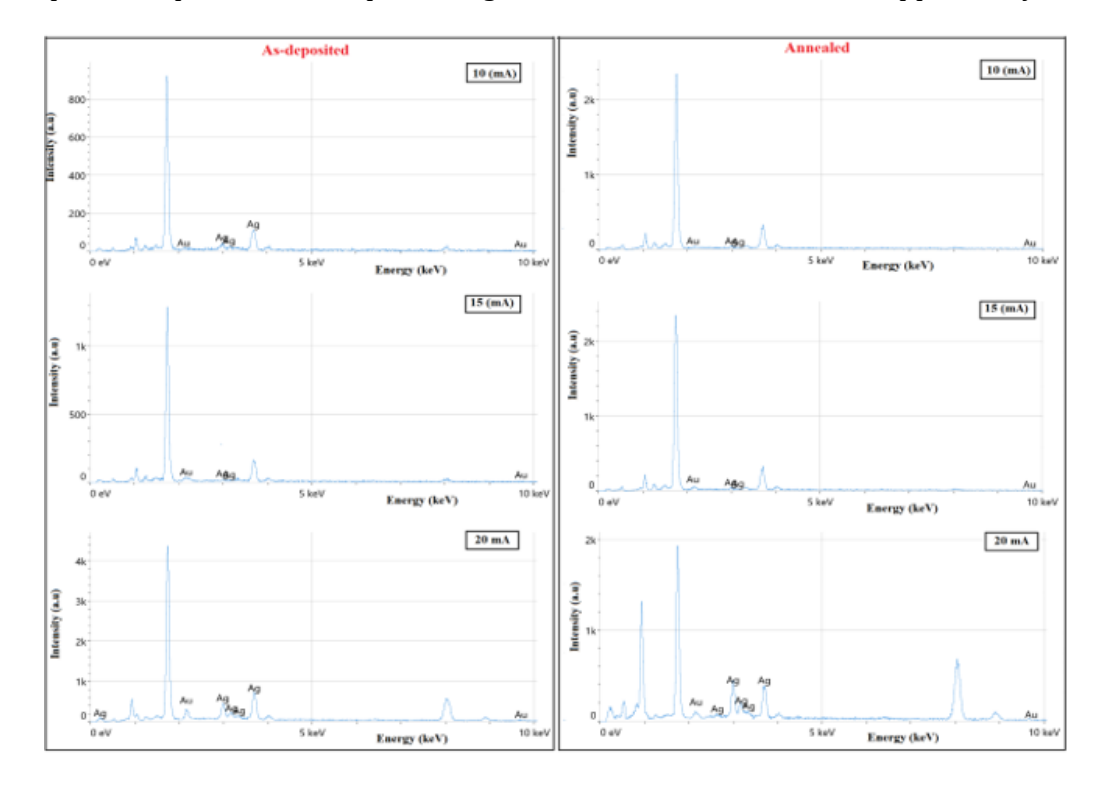


Figure 7: EDX analysis of as-deposited and annealed Ag/Au thin films deposited at different sputtering currents

Table 2 lists the elemental analysis of Au and Ag content for each case, including the weight percentage and atomic percentage. The Au content was lower than Ag for all samples, which attributed to the difference in sputtering yield between the two metals under the same conditions, as their difference in their binding energy [17]. This result is consistent with previous study using a 1:1 Ag/Au target, the percentage of gold was only 10% in the sputtered film

[18]

It was also observed that the Au percentage increased with increasing sputtering power, as a result of providing sufficient energy to the Au atoms to be sputtered, results more gold-rich films. This change in the film composition affects its structural, electrical, and optical properties, and thus its potential applications.

Table 2: EDX analysis of Ag/Au thin films deposited using different sputtering currents at 2 and 4 mbar, and of the annealed samples

P (mbar)	Annealing	Current (A)	Element	Atomic %	Weight %
2	As-deposited	10	Ag	90.2	83.4
			Au	9.8	16.6
		15	Ag	88.3	80.4
			Au	11.7	19.6
		20	Ag	71.8	58.3
			Au	28.2	41.7
2	Annealed	10	Ag	87.8	81.2

			Au	12.2	18.8
		15	Ag	83.6	73.7
			Au	16.4	26.3
		20	Ag	74.3	60.3
			Au	25.7	39.7

The optical properties of Ag:Au thin films deposited at different sputtering currents (10, 15, and 20 mA) were studied using UV-Vis absorption. Figure 8 show the absorption spectra of as-deposited and annealed Ag:Au thin films deposited on glass substrates using different sputtering currents. The absorbance spectra showed a decrease with increasing wavelength for all sputtering currents, with maximum values in the UV region (at wavelengths below 400 nm) and then decreasing toward the visible and near-infrared regions. The absorption edge was unclear when deposited at 2 mbar without annealing, which attributed to an incompletely connected grain structure with a high defect density. However, annealing significantly increased the optical absorbance, revealing a clear absorption edge due to improved crystallinity and the removal of crystalline defects, as demonstrated by XRD.

The absorption spectra of the annealed samples show that a wide band can be observed around 400 nm and this corresponds to the Localized Surface Plasmon Resonance (LSPR) of the Ag nanoparticles since it has a higher content more than Au. This band is even more intense at 10 mA sputtering currents because the additional contribution at that level is the nanosized Ag particles that are the best supporters of LSPR at this wavelength. The plasmon band intensity is slowly lowered as the current of sputtering increases. This decrease may be attributed to the evolution of the particle size, which is reported in by FESEM images..

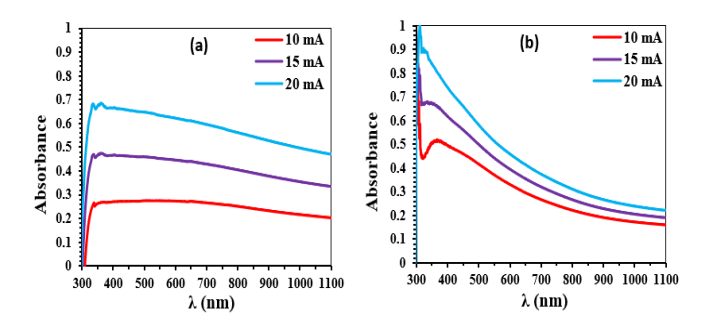


Figure 8: UV-visible absorbance of as-deposited and annealed Ag/Au thin films deposited at different sputtering currents

4. Conclusion

The experiment showed that structural, morphological and element composition of Ag/Au films can be fine-tuned by manipulating the sputtering conditions in addition to annealing. including the sputtering current. Continuous or further heating was also demonstrated to be a choice to get the good crystallinity and uniform surfaces. XRD analysis proved that the deposited films progressively change anisotropic characteristics at 10 mA to compact angle grains at 20 mA, which depict additional atomic mobility and growth mechanisms by the stronger sputtering power leading to increased grain size. Optimisation results into higher crystallinity and minimised structural defects. It improves the overall structural ordering of the as-deposited films and thus is shown to enhance the crystalline quality obtained in the deposition process and so works in conjunction with the high current sputering as well as the post-deposition annealing in enhancing alloying, grain growth and lattice relaxation in Ag/Au thin films. The morphological investigations by FESEM revealed that under these conditions, a uniform distribution of nanoparticles with a moderate amount of surface roughness is attained. These findings indicate that a combination of accurate sputtering parameters and heat treatment is an appropriate approach in the high quality in films in terms of both structure and performance, which is useful in the design of Ag/Au thin films to be used in optoelectronics, sensors, and nanodevices...

References

[1]A. Ajith, M.N.S. Swapna, H. Cabrera, S.I. Sankararaman, Comprehensive Analysis of Copper Plasma: A Laser-Induced Breakdown Spectroscopic Approach, Photonics. 10 (2023). https://doi.org/10.3390/photonics10020199.

[2]S.T. Hsieh, H. Mishra, N. Bolouki, W. Wu, C. Li, J.-H. Hsieh, The Correlation of Plasma Characteristics to the Deposition Rate of Plasma Polymerized Methyl Methacrylate Thin Films in

- an Inductively Coupled Plasma System, Coatings. 12 (2022) 1014. https://doi.org/10.3390/coatings12071014.
- [3]J.H. Bae, L.B. Bayu Aji, S.J. Shin, A.M. Engwall, M.H. Nielsen, A.A. Baker, S.K. McCall, J.D. Moody, S.O. Kucheyev, Gold-tantalum alloy films deposited by high-density-plasma magnetron sputtering, J. Appl. Phys. 130 (2021). https://doi.org/10.1063/5.0050901.
- [4]M.O. Salman, W.A.A.R. Khalaf, B.O. Ahmed, Comparison between plasma distribution in plane and concave cathodes DC discharge systems, J. Theor. Appl. Phys. 18 (2024). https://doi.org/10.57647/j.jtap.2024.si-AICIS23.19.
- [5]M. Islam, Z. Matouk, N. Ouldhamadouche, J.-J. Pireaux, A. Achour, Plasma Treatment of Polystyrene Films—Effect on Wettability and Surface Interactions with Au Nanoparticles, Plasma. 6 (2023) 322–333. https://doi.org/10.3390/plasma6020022.
- [6]Y. Chen, D. Shi, Y. Chen, X. Chen, J. Gao, N. Zhao, C.P. Wong, A facile, low-cost plasma etching method for achieving size controlled non-close-packed monolayer arrays of polystyrene nano-spheres, Nanomaterials. 9 (2019). https://doi.org/10.3390/nano9040605.
- [7]A. le Febvrier, L. Landälv, T. Liersch, D. Sandmark, P. Sandström, P. Eklund, An upgraded ultrahigh vacuum magnetron-sputtering system for high-versatility and software-controlled deposition, Vacuum. 187 (2021) 110137. https://doi.org/https://doi.org/10.1016/j.vac uum.2021.110137.
- [8]G.L. Stansfield, H.M. Johnston, S.N. Baxter, P.J. Thomas, Deposition of Ag and Ag-Au nanocrystalline films with tunable conductivity at the water-toluene interface, RSC Adv. 8 (2018) 6225–6230. https://doi.org/10.1039/c7ra13370g.
- [9]C. Surya Prakasarao, P. Hazarika, S.D. DSouza, J.M. Fernandes, M. Kovendhan, R. Arockia Kumar, D. Paul Joseph, Investigation of ultra-thin and flexible Au–Ag–Au transparent conducting electrode, Curr. Appl. Phys. 20 (2020) 1118–1124.
 - https://doi.org/10.1016/j.cap.2020.06.016.
- [10]D. Kim, J. Nam, B.J. Lee, Plasmon thermal conductivity of thin Au and Ag films, Phys. Rev. B. 108 (2023) 205418.

- https://doi.org/10.1103/PhysRevB.108.20541 8.
- [11]S. Yergaliyeva, R. Nemkayeva, N. Guseinov, O. Prikhodko, A. Arbuz, B. Orynbay, Y. Sagidolda, M. Aitzhanov, G. Ismailova, Y. Mukhametkarimov, Synthesis and optical properties of Ag/Au-TiO2 plasmonic composite thin films, Opt. Mater. Express. 13 (2023) 2726–2736. https://doi.org/10.1364/OME.495430.
- [12] W.H. Bragg, W.L. Bragg, X Rays and Crystal Structure, G. Bell and Sons, LTD., London, 1918.
- [13]D.R.A. El-Hafiz, M.A. Ebiad, A.A.E. Sakr, Ultrasonic-Assisted Nano-Nickel Ferrite Spinel Synthesis for Natural Gas Reforming, J. Inorg. Organomet. Polym. Mater. 31 (2021) 1–10. https://doi.org/10.1007/s10904-020-01718-z.
- [14]M.A. Hammadi, Rare Earth Additive Effect on Sensing Behavior of ZnO/PS Nanostructure, University of Anbar, 2013.
- [15]C.O. Duya, F.O. Okumu, M.C. Matoetoe, The electrochemical properties of bimetallic silvergold nanoparticles nano film's., Heliyon. 10 (2024) e36974. https://doi.org/10.1016/j.heliyon.2024.e36974.
- [16]N. Mancini, E. Rimini, Annealing of polycrystalline Au and Au-Ag thin films, Surf. Sci. 22 (1970) 357–364. https://doi.org/10.1016/0039-6028(70)90088-9.
- [17]S.S. Johar, D.A. Thompson, Spike effects in heavyion sputtering of Ag, Au and Pt thin films, Surf. Sci. 90 (1979) 319–330. https://doi.org/10.1016/0039-6028(79)90346-7.
- [18]P. Sangpour, O. Akhavan, A.Z. Moshfegh, The effect of Au/Ag ratios on surface composition and optical properties of co-sputtered alloy nanoparticles in Au-Ag:SiO2 thin films, J. Alloys Compd. 486 (2009) 22–28. https://doi.org/10.1016/j.jallcom.2009.06.20 1.
- [19] Jam, F. A., Singh, S. K. G., Ng, B. K., & Aziz, N. (2018). The interactive effect of uncertainty avoidance cultural values and leadership styles on open service innovation: A look at malaysian healthcare sector. International Journal of Business and Administrative Studies, 4(5), 208.